Ultrasonic Phased Array Device for Real-Time Acoustic Imaging in Air

Sevan Harput, Ayhan Bozkurt and Feysel Yalcin Yamaner

Acoustic Group. Sabanci University, Faculty of Engineering and Natural Sciences

Orhanli-Tuzla, 34956 Istanbul, Turkey.

Abstract—A real-time acoustic imaging system is developed as a prototype electronic travel aid (ETA) device. The design is implemented on a field programmable gate array (FPGA). A 6 channel transmit and 4 channel receive digital beamforming algorithm with dynamic focusing is accommodated in a FPGA. The developed system consists of a FPGA, pulser and receiver circuitry and separate transmitter and receiver arrays, which are constructed by using commercially available transducers. The transducer elements have a physical dimension of 1.9 wavelengths and a half-power beamwidth of $43°$ at 40.8 kHz center frequency. The transmitter array is formed by aligning the transducers with minimum spacing between the elements, which is 2 wavelengths. Obviously, more than one wavelength inter-element spacing leads to the occurrence of grating lobes in the array response and decreases the Field of View (FOV) below the half-power beamwidth of transducers. To extend the FOV and eliminate the grating lobe, the receiver array is formed with 3 wavelength inter-element spacing. The non-identical element spacing makes the grating lobes of transmitter and receiver array to appear at different places. The described placement strategy and the functionality of the system is tested with several experiments. The results of these experiments prove the grating lobe suppression capability of the applied placement strategy.

I. INTRODUCTION

Phased array principles have not been extensively applied for acoustic imaging in air. In this work, the design and experimental verification of an ultrasonic phased array system for real-time acoustic imaging in air is presented. The developed device uses phase beamforming technique [1] to electronically sweep the acoustic beam and produce a sector scan for the detection of proximate objects [2]. The intended application of the device is giving mobility aid to visually impaired people. Therefore, compactness and low power consumption are important design criteria. The device is built using 6 transmitter and 4 receiver elements and has an angular resolution of $4.23°$.

Among recently developed ETA devices, the most popular two devices are "Navbelt" [3] and "GuideCane" [4]. The working principle of both devices is based on array structure; without scanning the environment, each transducer element collects data from a single angle [5]. A recent device that uses the phased array technique is an ultrasonic obstacle detector introduced by Strakowski, Kosmowski, Kowalik, and Wierzba in 2006 [6]. The developed device only performs receive beamforming by using a single ultrasound source and an array of microphones.

Non of the pre-developed devices use the phased array principle completely. Phased arrays has numerous advantages over single-element imaging systems, but it requires an inter-element spacing (*i.e.* the distance between the centers of two adjacent elements) to be less than one wavelength in order to fully suppress the grating lobes. However, the transmitter array is formed with 2 wavelengths spacing between the elements. As expected, this placement leads to the occurrence of unwanted grating lobes in the array response and decreases the FOV to $30°$. By using a spacing of 2 wavelengths, the FOV of the overall system can not be larger than $±15°$ with identical receiver and transmitter arrays. For this reason, the receiver array elements are placed with a different spacing. Forming the receiver and transmitter arrays with non-identical element spacing makes the grating lobes to appear at different places. For 3 wavelengths inter-element spacing in receiver array, the first grating lobe of the overall system moves to $±30°$ and the FOV increases to $60°$. This value exceeds the limit imposed by the half-power beamwidth of an individual transducer element and makes the grating lobes to appear outside of the active imaging area.

The described design has been implemented on a FPGA clocked at 50 MHz. A 6 channel transmit and 4 channel receive digital beamforming algorithm is accommodated in a FPGA. In order to obtain better results from the developed imaging system, the design is applied with dynamic focusing in transmit and receive. Due to high clock rates, flexibility, parallel processing ability and reprogrammability of the FPGA, a real-time partial delay-sum beamforming algorithm can be implemented for the receive beamforming.

II. ARRAY CONFIGURATION

The ultrasonic phased array device is constructed using commercially available transducers with the specifications shown in Table I. Each transducer elements have a radius of 1.9 wavelengths and a half-power beamwidth of $43°$ at 40.8 kHz center frequency. The transmitter array is constructed with 6 elements and 2λ inter-element spacing. The element spacing larger than the Nyquist distance causes grating lobes inside the imaging area. If identical receiver and transmitter arrays were used, the FOV would be limited with $30°$, which is the angular spacing between the main beam and the first grating lobe. However, the selected transducer elements can be used for a scanning range of $43°$ (Table I), which is larger than the $30°$ limit for the FOV imposed by the array configuration. Scanning beyond the $30°$ will result in ghost objects in the

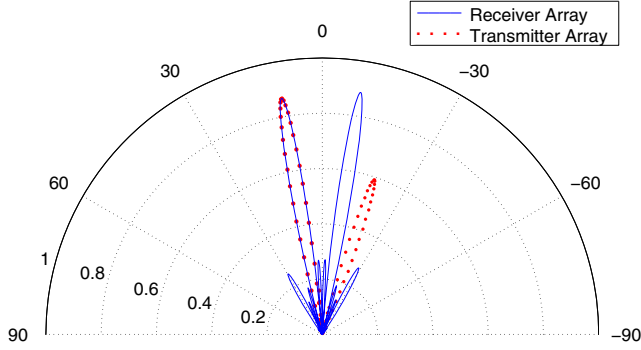| MANUFACTURER	Pro-Wave Electronic Corp., Taiwan.
TYPE	400ST/R160 (piezoelectric)
FREQUENCY	40.8 kHz
PHYSICAL SIZE	16 mm (1.9λ)
HP BEAMWIDTH	43°

Fig. 1. Directivity patterns of the transmitter and receiver arrays, which are focused to 10°. Transmitter array is formed with 6 elements and $d = 2\lambda$. Receiver array is formed with 4 elements and $d = 3\lambda$. The main beams of the both arrays are entirely overlap, but the grating lobes are not overlapping with each others.

Fig. 2. Picture of the developed phased array device showing the transmitter and receiver arrays.

Fig. 3. Picture of the developed system.

image, if the same array configuration is used for receiving.

In order to eliminate the effect of the grating lobe in the transmitter array response, the inter-element spacing of receiver array is adjusted with a different strategy. The grating lobe of the transmitter array is aligned with one of the nulls of the receiver array response. After solving the necessary equations mentioned by S. Harput and A. Bozkurt in [7], the receiver array is formed with 3λ inter-element spacing and 4 elements.

The 2λ inter-element spacing limits the FOV of the overall system to ±15° for identical receiver and transmitter arrays. Setting inter-element spacing of the receiver array to 3λ moves the first grating lobe of the overall system to ±30°.

Fig. 1 shows the transmit and receive directivity patterns when both arrays are focused to 10°. The directivity pattern of the overall system is the product of the directivity patterns of the transmitter and receiver arrays. This is also referred to as *pattern multiplication* for arrays of identical elements [8]. Pattern multiplication causes the grating lobes of transmitter and receiver array to disappear and consequently increasing the FOV to 60°. This value exceeds the limit imposed by the half-power beamwidth of an individual transducer element and makes the grating lobes to appear outside of the active imaging area.

After analyzing the directivity patterns above, the receiver and transmitter arrays are constructed with the mentioned placement strategy. Two linear arrays are realized by using the transducers with the features shown in Table I. Fig. 2 shows a picture of the constructed arrays.
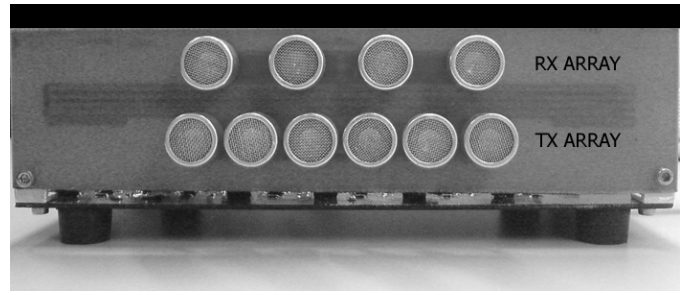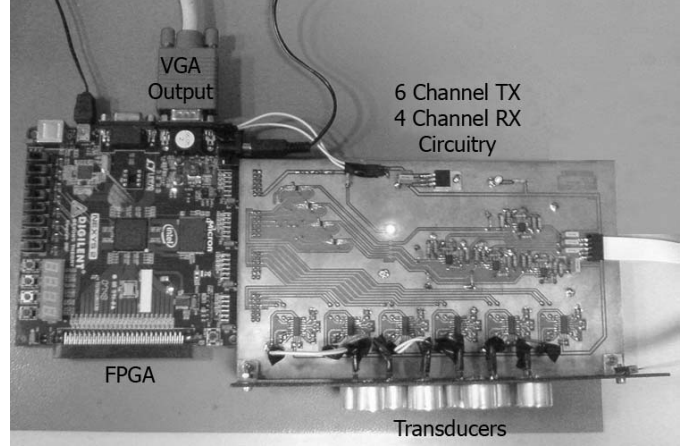
III. SYSTEM HARDWARE

The developed system consists of a receiver array, a transmitter array, a printed circuit board for 6 channel pulser and 4 channel receiver circuitry, a Video Graphics Array (VGA) monitor for displaying the image, and a Digilent Nexys2 Board (Digilent Inc., Pullman, WA). The FPGA board works with a 50 MHz clock and has a Spartan3E-500 FG320 Xilinx FPGA chip (Xilinx Inc., San Jose, CA) on it, which is directly connected to a 16 MB Micron M45W8MW16 Cellular RAM (Micron Technology Inc., Boise, Idaho). The Nexys2 Board also has a 8-bit VGA output for the applications, which need a display. The picture of the developed system is shown in Fig. 3.

A. Transmit and Receive

The designed device has separate transmitter and receiver arrays. This scheme decreases the complexity of pulser and receiver circuitry, but increases the number of transducers. The pulser circuit is directly triggered by the signal from the FPGA. The 6 channel pulser circuit amplifies the coming signal and generates a ±12 volt driving signal for transducers in the transmitter array.

The 4 channel readout circuitry amplifies and filters the received echo and sends it to the A/D converters. The digital beamformer simultaneously gets the digitized data from 4 different A/D converters. As a rule of thumb, it is required

to achieve a $4 - 10$ times higher sampling frequencies than the array frequency [9], but in this application each channel is digitized at 780 kSps, which results in an oversampling ratio of approximately 19. The oversampling of the echo decreases the complexity of the beamformer by eliminating the need for interpolation or a fine/coarse delay strategy. The oversampling allows the delay of the beam data to be implemented at integer multiplies of the sampling rate with a high accuracy, but it increases the amount of data to be stored. The storage problem is solved by using a partial delay-sum algorithm. The maximum required time delay between the transducers is calculated and the size of the input buffers is determined. With this strategy, the received data is summed partially and stored in the random-access memory (RAM) on the FPGA after downsampling.

B. FPGA Impelentation

The transmit and receive beamforming algorithms are coded in Verilog, synthesized and loaded into a FPGA. By using beamforming principle, the system transmits acoustic pulses through 6 different channels and receives simultaneously from 4 different channels at 780 kHz sampling frequency with 12-bit precision. The received echo signal is digitized by a AD7274 A/D converter (Analog Devices Inc., Norwood, MA) and processed with a partial delay-sum beamforming algorithm, which is implemented on a FPGA.

After receive beamforming the processed data is written in the off-chip RAM on the FPGA board. The stored data in the RAM is monitored on a 640×480 computer screen. The 16 MB SDRAM on the FPGA board is used for storage rather than the on-chip memory blocks in the FPGA chip. The on-chip memories work faster than off-chip memories, however most FPGA chips have architectures with small size on-chip memory blocks, which are mostly used as buffer memory.

The 16 MB Micron M45W8MW16 Cellular RAM has a random access time of 70 ns. In synchronous mode the RAM can make a burst read with a latency of 20 ns, but asynchronously reading or writing in 20 ns (one clock cycle) is impossible. For this reason, a VGA *blank* signal is generated in compliance with the $640 \times 480 \times 60$ Hz industrial VGA standard. The horizontal scan line has 640 pixels for video, but it has 800 pixels total per line. Hence, the *blank* signal duration is $(800 - 640)/25$ MHz $= 6.4\mu$s, which is the free time between each horizontal scan lines. During this period, there is no need to read the RAM to update the VGA frame. Instead the processed data by RX module is written to RAM without affecting the refresh rate of VGA.

The block diagram of the FPGA implementation for ultrasonic phased array device shows the behavioral model of the system as shown in Fig. 4. First the TX module calculates the necessary time delays for a predetermined beamforming angle. It starts to send the driving signal to the transmit circuitry for 6 transducer elements. After finishing one transmit cycle, the TX module waits 20 ms for RX module to capture the returning echo. When 20 ms passes, the RX module stops receiving digitized signal from A/D converter and TX module starts to
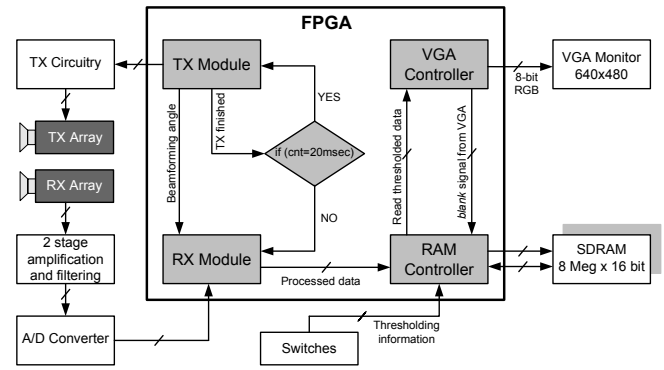

Fig. 4. Behavioral model of the system.

TABLE II
EXPERIMENTAL PARAMETERS

PARAMETER	VALUE
SCANNING RANGE	0.2m to 3.3m
FIELD OF VIEW	40°
SAMPLING ANGLE	$\Delta\theta = 4°$
WORKING FREQUENCY	f = 40.8 kHz
ADC SAMPLING SPEED	780 kSps
PULSE WIDTH	8 cycles (196 μsec)

pulse the TX array for a different beamforming angle. Meanwhile, the VGA controller always reads the RAM to update the image on the screen of a VGA monitor. RAM Controller module checks the *blank* signal from VGA Controller and directly writes or buffers the processed data coming from RX module. RAM controller also performs the thresholding by reading the current state of the manually controlled switches outside the FPGA.

IV. EXPERIMENTS

To measure the performance of the developed phased array device, experiments are performed on a set of objects with various shapes placed at different locations. During the experiments transmit and receive beamforming is performed in a range of $-20°$ to $20°$ with an angular resolution of $4°$. The sampled echo by the A/D converter is transferred to the FPGA and the receive beamforming is done by the implemented partial delay-sum beamforming algorithm. Finally, the FPGA outputs the angular and distal information to VGA monitor screen.

While forming the final image, the beamformed data is not converted form polar coordinates to Cartesian coordinates. Since the developed system is a prototype of an ETA device, it can be used to guide a visually impaired person and the final data is not needed to be expressed as a medical ultrasound image. The distal and angular information of the present object/objects are sufficient to perform mobility aid for visually impaired people.
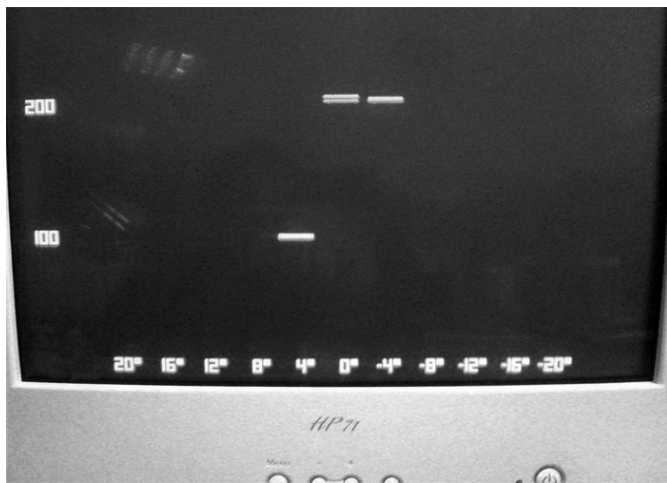
Fig. 5. Experiment-I. First object is placed 105 cm away from the device with an angle of $5°$. Second object is placed 210 cm away from the device with an angle of $-3°$. The image has 21 dB dynamic range.

Fig. 6. Experiment-II. A good reflector is placed 150 cm away from the device with an angle of $20°$. A bad reflector is placed 120 cm away from the device with an angle of $-12°$. The good reflector appears brighter and the bad reflector appears dimmer in the image. The image has 21 dB dynamic range.

A. Experiment I

Two different wooden blocks are used in this experiment because of their high reflectivity. A 10 cm wide block is placed 105 cm away from the device with an angle of $5°$. Another block with a 40 cm width is placed at $-3°$ with a distance of 210 cm. Both objects are detected successfully and they can be easily separated from each other as seen in Fig. 5. It can be seen from the figure that an object is located at 105 cm from the device and with an angle of $4°$. The angular resolution of the system is $4°$, any objects appears between $4° - 7°$ will be treated as $4°$.

The second object is located at 210 cm from the device and it appears in $0°$ and $-4°$. Since the object has a bigger lateral surface, it covers both of the angles.

B. Experiment II

Two different are used in this experiment with different reflectivity. A 10 cm wide wooden block is placed 150 cm away from the device with an angle of $20°$. A bad reflector is placed at $-12°$ with a distance of 120 cm. Both objects are detected with different intensities as seen in Fig. 6. The wooden object appears brighter in the image because of its higher reflectivity. The bad reflector is also detected successfully, but it is seen dimmer in the image.

In both of the experiments the exact shape of the objects can not be determined. Although the resolution is poor, the collected object data can give the user enough information to avoid the obstacles.

V. CONCLUSION

In this work, the FPGA implementation and experimental verification of a real-time ultrasonic imaging system is presented. The usage of commercial transducers makes the receiver and transmitter array to have an inter-element spacing of more than a wavelength, which results in grating lobes

in array pattern. This problem was solved by forming the transmitter array with 2λ and receiver array with 3λ inter-element spacing, and the FOV was extended to $60°$. The experimental results prove that the applied placement strategy for the array elements successfully suppresses the grating lobes.

Developed device scans the imaging area using the phased array technique with an angular resolution of $4.23°$. To achieve the same angular resolution without scanning will be more costly. An array would require approximately the same number of transducers but individual elements have to be as wide as the aperture size of the phased array. For this reason, the developed phased array device is more compact than an array of transducers.

REFERENCES

[1] O. T. V. Ramm and S. W. Smith, "Beam steering with linear arrays," *IEEE Trans. Biomed. Eng.*, vol. BME-30, no. 8, pp. 438–452, 1983.
[2] K. Higuchi, K. Suzuki, and H. Tanigawa, "Ultrasonic phased array transducer for acoustic imaging in air," in *IEEE Ultrasonics Symposium*, 1986, pp. 559–562.
[3] S. Shoval, J. Borenstein, and Y. Koren, "Mobile robot obstacle avoidance in a computerized travel aid for the blind," in *IEEE International Conference on Robotics and Automation*, vol. 3, 1994, pp. 2023–2028.
[4] J. Borenstein and Y. Ulrich, "The guidecane-a computerized travel aid for the active guidance of blind pedestrians," in *Proc. IEEE International Conference on Robotics and Automation*, vol. 2, 1997, pp. 1283–1288.
[5] S. Shoval, J. Borenstein, and Y. Koren, "Navbelt and the guide-cane [obstacle-avoidance systems for the blind and visually impaired]," *IEEE Robot. Autom. Mag.*, vol. 10, no. 1, pp. 9–20, 2003.
[6] M. Strakowski, B. Kosmowski, R. Kowalik, and P. Wierzba, "An ultrasonic obstacle detector based on phase beamforming principles," *IEEE Sensors J.*, vol. 6, no. 1, pp. 179–186, 2006.
[7] S. Harput and A. Bozkurt, "Ultrasonic phased array device for acoustic imaging in air," *IEEE Sensors J.*, submitted for publication.
[8] C. A. Balanis, *Antenna Theory*, 3rd ed. Wiley-Interscience, 1997, ch. Arrays: Linear, Planar, and Circular, pp. 283–320.
[9] B. D. Steinberg, "Digital beamforming in ultrasound," *IEEE Trans. Ultrason., Ferroelectr., Freq. Control*, vol. 39, pp. 716–721, 1992.